A Digital Calorimeter for Dark Matter Search in Space

Journal of Physics: Conference Series **293** (2011) 012038 doi:10.1088/1742-6596/293/1/012038

A Digital Calorimeter for Dark Matter Search in Space

X L Sun[1], J G Lu[1], T Hu[1], L Zhou[1], X Cai[1], B X Yu[1], J Fang[1], Y G Xie[1], Z H An[1], Z G Wang[1], A W Zhang[1], Z Xue[1]

[1]Institute of High Energy Physics, Beijing, China

E-mail:sunxl@ihep.ac.cn

Abstract. A novel digital imaging calorimeter is designed for the observation of high energy electrons and gamma rays on the Space Station of China. The MC data shows that the calorimeter has a capability of observing the electrons (without separation between e+ and e-) and the gamma-rays in 30GeV-5TeV with a high energy resolution of 4% over 500GeV, a good angular resolution of 0.5 degree over 500GeV, and a high proton rejection power of ~$5x10^5$(95% signal efficiency). The calorimeter has a large geometrical factor of ~3.3 m^2sr (5 sensitive faces) with ~1T weight. The excellent energy resolution make us can detect any change of the energy spectra and a line signature in the energy distribution, as expected from the dark matter.

1. Introduction

WMAP data reveals that dark matter comprises 23% of the universe [1]. This matter, different from atoms, does not emit or absorb light. It has only been detected indirectly by its gravity such as the rotation curves of galaxies, strong gravitational lenses and weak gravitational lenses. There are some candidates in particle physics: Stable weakly interacting massive particles (WIMPs) of mass 10GeV-10TeV, Massive neutrinos, Axions, Kaluza Klein particles, etc. WIMPs is preferred by most of theorist, which occur in several well-motivated theories beyond the Standard Model such as Supersymmetry, Inert Higgs models, etc. There are two detection mechanisms of WIMPs: Direct detection, detect signal of DM collisions with nuclei; Indirect detection, detect final decay products ($e^{\pm}, \gamma, p, \bar{p}, \nu$) of DM annihilation. Line signature from DM annihilation to double gamma-rays is the decisive evidence of DM. Dark matter search in space is an important method of indirect detection. Excellent capability of proton rejection with power ~10^5 is necessary for identifying electrons and gamma-rays in space because electron is about 10^{-2}-10^{-3} of proton and gamma-ray is about 10^{-3}-10^{-6} of proton between 30GeV-10TeV. Space Station of China will be built at 2020, a payload for dark matter search is proposed by IHEP. The detector should have capabilities:

- Energy range: 30GeV-5TeV (cover WIMP mass range)
- Energy resolution: < 5% (detect line signature requirement)
- Background rejection power: > 10^5 (suppress proton background requirement)
- Total power: < 500 Watts
- Total mass: < 1.5 Tons

2. Detector design

2.1 Detector concept design

The detector has two chief components: Anti-Coincidence Detector (ACD) and Digital Imaging Calorimeter (DIC). ACD is a positional sensitive plastic scintillator detector in order to reject charged particles for the gamma-rays observation. DIC is a 3D crystal array. Each crystal is a little cube with one face coupled with WLS fiber which collect and guild photons to ICCD camera. All separate cubes are glued together. "Digital" means hit mark '1', and non-hit mark '0' for each crystal. All the '01' describe the shower's image. We can get the information of particle energy, particle type and incident angle by the analysis of image.

2.2 ACD structure

ACD is composed of $1\times1\times80$ cm plastic scintillator array along x and y direction, which covers more than 5/6 of the main body. Each scintillator has a WLSF inbuilt in a groove on surface. Reading out devoice is SiPM. ACD is positional sensitive, so the incident position of charged particle can be got associated with the shower axis in DIC.

2.3 Trigger structure

One fiber attached the surfaces of one string of crystals, and all fibers coupled with one PMT. When a high energy particle inject, we can get a fast signal (<100ns) which directed proportion the particle energy. So a threshold can be set for trigger.

2.4 Chief feature of the design

- Digital image means there is no problem of the amplitude saturation.
- 5 sensitive faces mean a large field of view.
- High level of granularity means good particle identify power and good angle resolution.
- CCD reading out means low power ~30 watts.
- ACD is positional sensitive, which means high suppress for backflash [2] charged particles.

3. MC simulation study on performance

3.1 Detector geometry

Total length is 60cm (~32 r.l.), and the side length of little crystal cube is 1.5-4.5cm. There is 1mm glue interval between two crystals. The code is written with GEANT4, physics list is QGSP. Digital energy cut is 12MeV (muon MIP deposit energy) for each crystal.

3.2 Relationship between incident energy and number of hit crystals

From the MC data we found the relationship is:

$$N_{hit}^2 \propto E_{incident} \tag{1}$$

As can be seen from figure 1, linear relationship is good at high energy range and a little worse at low energy range.

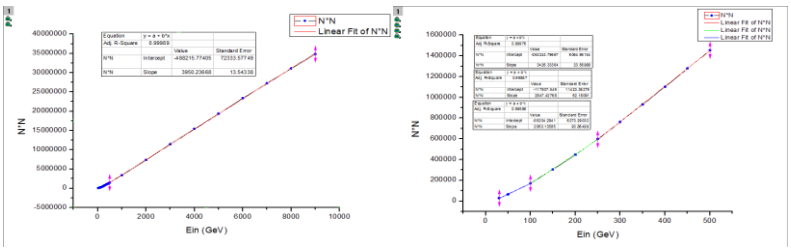

Figure 1. Relationship between incident energy and number of hit crystals.

3.3 Energy resolution

According to the relationship (1), we can get the energy reconstruction. Figure 2 is energy reconstruction of 1000GeV gamma-rays inject. The energy resolution is 3.27%. Figure 3 is energy resolution compare with different granularity 1.5-4.5 cm. About 4% can be reached above 500GeV.

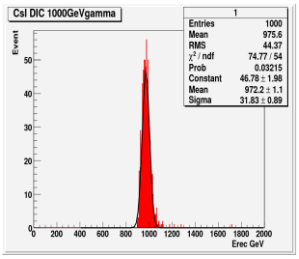

Figure 2. Energy reconstruction of 1000GeV gamma-rays.

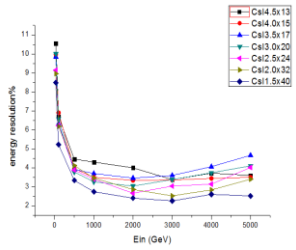

Figure 3. Energy resolution compare of different granularity 1.5-4.5 cm.

3.4 Angular resolution

Position and angular of incident particle can be got from shower axis reconstruction. Figure 4 shows shower axis reconstruction, figure 5 is position and angular distribution of incident particle, figure 6 is angular resolution compare with different angularity 1.5-4.5 cm. About 0.5° can be reached over 500GeV.

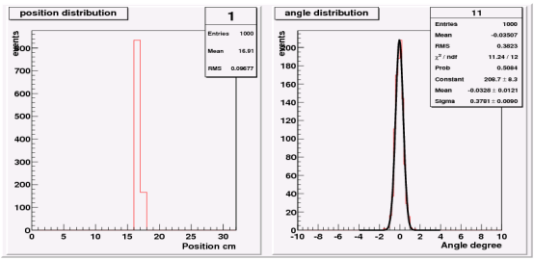

Figure 5. Position and angular distribution of incident particle.

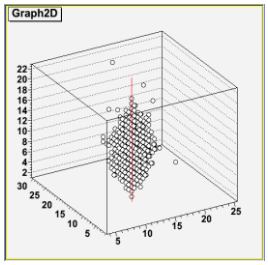

Figure 4. Shower axis reconstruction.

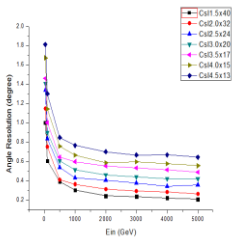

Figure 6. Angular resolution compare of different angularity 1.5-4.5 cm.

3.5 Particle identification

3.5.1 Gamma-ray proton separation There are two main differences between proton shower and gamma-ray shower:

- Proton induced showers are longitudinally wider than electron showers because of the spread of secondary particles.
- Gamma-ray induced showers will start and die off earlier than proton showers.

Figure 7 and figure 8 show the differences clearly.

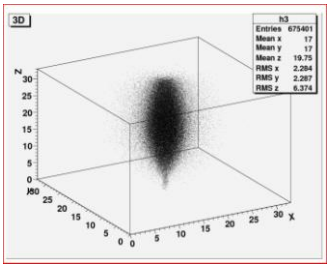

Figure 7. 3D image of electron shower.

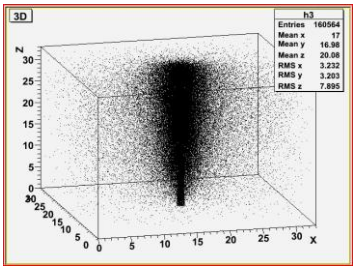

Figure 8. 3D image of proton shower.

A separation is done with TMVA tool in root. The input is:

- Signal: gamma-ray, 100GeV, 140000 events.
- Background: proton, 100GeV-5000GeV with power law 2.7, 1M events.

Figure 9 shows the output: proton rejection power is about 5×10^5, signal efficiency is 95% and BDT method has a better performance.

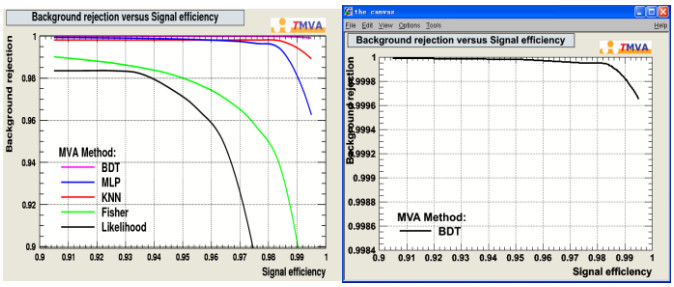

Figure 9. Background rejection versus signal efficiency.

3.5.2 Gamma-ray electron separation Difference is electron shower starts earlier than gamma-ray shower. A separation is done with TMVA, the input is:

- Signal: gamma-ray, 100GeV, 140000 events.
- Background: electron, 100GeV, 160000 events.

Figure 10 shows the output: electron rejection power is about 1×10^4,signal efficiency is 45% and BDT also has a better performance.

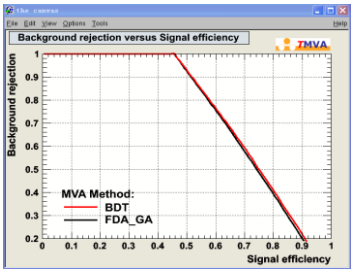

Figure 10. Background rejection versus signal efficiency.

4. Prototype study

4.1 Unit structure

The crystal side length is 2.5cm packing ESR, the WLS fiber plate attaching to one face of the crystal is the key structure for light reading out. Figure 11 is the unit structure.

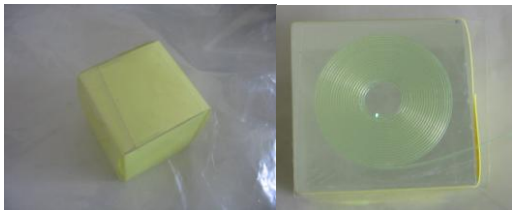

Figure 11. Unit structure.

Muon test is done for unit structure with different crystals. Figure 12 is view of the test system. We found CsI(Na) has the best light output about 188 photoelectrons for muon MIP signal. Figure 13 is the spectrum of muon MIP signal. Figure 14 is light output comparing with different crystals.

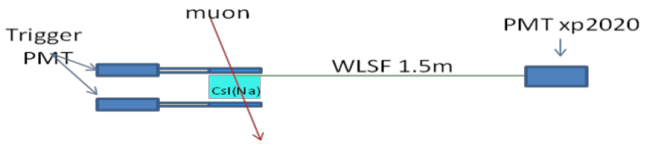

Figure 12. View of muon test system.

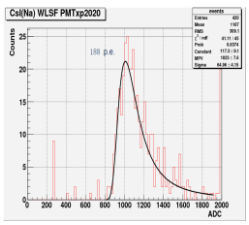

Figure 13. Spectrum of moun.

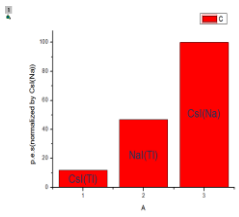

Figure 14. Light out of different crystals.

4.2 Prototype array

A prototype of 2×2×6 array is made for moun test. Figure 15 is schematic view of the muon test system.

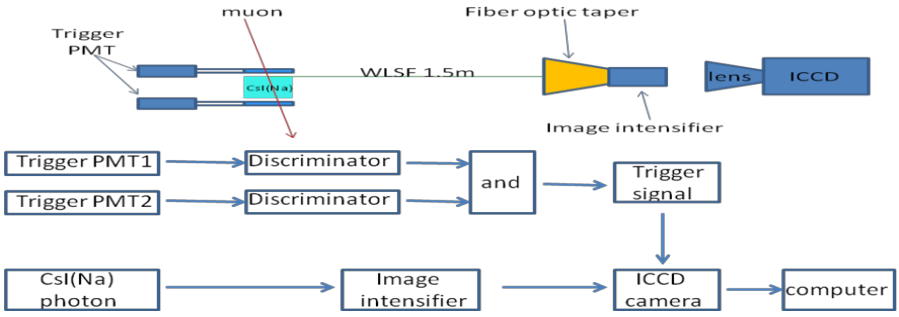

Figure 15. Schematic view of the muon test system.

Image intensifier is necessary, its key effective is: intensified image; photon delay for waiting trigger. Figure 16 is a ICCD photo of a muon event. The signal is clear and the ratio of signal to noise is about 8.

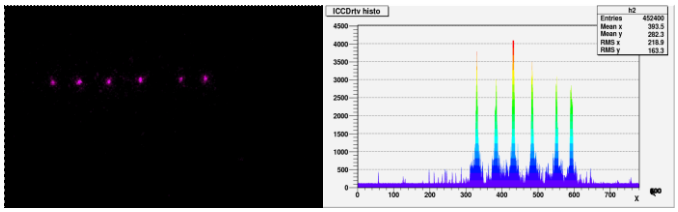

Figure 16. ICCD photo of a muon event.

4.3 Capacity analysis

Magnification of FOT and size of CCD are the key factors for capacity. For Φ300um fiber with 100um interval and 450000 pixels CCD, the relationship between magnification and capacity is shown in table 1.

Table 1. Relationship between magnification and capacity.

Magnification	Capacity(fibers)
2:1	4500
3:1	10000
4:1	18000
5:1	28000

Capacity 28000 can cover a 30×30×30 array, so only one CCD system needed for the whole calorimeter.

5. Summary

A scheme of 60cm cube CsI(Na) array is proposed: 5 faces sensitive, digital image, 32 radiation length, weight 1 ton, cover 30GeV to 5TeV energy range. The preliminary simulation is done: gamma proton separation power is 5×10^5 with 95% efficiency, electron proton separation power is 1×10^4 with 45% efficiency, energy resolution is 4% and angular resolution is 0.5^o. The prototype has been built and tested and the system has a good performance.

References

[1] Spergel D N *et al*. 2007 *Astrophys. J. Suppl. Ser.* **170**, 377
[2] Moiseev A A, Ormes J F, Hartman R C, Johnson T E, Mitchell J W and Thompson D J 2004 *Astropart. Phys.***22** 275